Eur. Phys. J. C 39, 87–94 (2005)
Digital Object Identifier (DOI) 10.1140/epjc/s2004-02081-2

THE EUROPEAN PHYSICAL JOURNAL C

The low-lying mass spectrum of the N = 1 SU(2) SUSY Yang-Mills theory with Wilson fermions

F. Farchioni[a], R. Peetz

Institut für Theoretische Physik, Universität Münster, Wilhelm-Klemm-Str. 9, 48149 Münster, Germany

Received: 14 September 2004 / Revised version: 29 October 2004 /
Published online: 21 December 2004 –

Abstract. We analyze the low energy spectrum of bound states of the N = 1 SU(2) SUSY Yang-Mills Theory (SYM). This work continues the investigation of the non-perturbative properties of SYM by Monte Carlo simulations in the Wilson discretization with dynamical gluinos. The dynamics of the gluinos is included by the Two-Step Multi-Bosonic Algorithm (TSMB) for dynamical fermions. A new set of configurations has been generated on a $16^3 \cdot 32$ lattice at $\beta = 2.3$ and $\kappa = 0.194$. The analysis also includes sets of configurations previously generated on a smaller ($12^3 \cdot 24$) lattice at $\kappa = 0.1925, 0.194$ and 0.1955. Guided by predictions from low energy Lagrangians, we consider spin-1/2, scalar and pseudoscalar particles. The spectrum of SYM is a challenging subject of investigation because of the extremely noisy correlators. In particular, meson-like correlators contain disconnected contributions. The larger time-extension of the $16^3 \cdot 32$ lattice allows to observe two-state signals in the effective mass. Finite-volume effects are monitored by comparing results from the two lattice sizes.

1 Introduction

The N = 1 SU(N$_c$) SUSY Yang-Mills (SYM) theory is the simplest instance of a SUSY gauge theory and presently the only one viable for large-scale numerical investigations. It describes N_c^2-1 gluons accompanied by an equal number of fermionic partners (gluinos) in the same (adjoint) representation of the color group. Veneziano and Yankielowicz [1] have shown how the assumption of confinement in combination with SUSY strongly constrains the low energy structure of the theory. The expected degrees of freedom dominating the low energy regime are composite operators of the gluon and gluino field which can be arranged into a chiral superfield. These are: the gluino scalar and pseudoscalar bilinears $\bar{\lambda}\lambda$, $\bar{\lambda}\gamma_5\lambda$, the corresponding gluonic quantities F^2, $\tilde{F}F$, and the spin-1/2 gluino-glue operator $\mathrm{tr}_c[F\sigma\lambda]$. However the program of including the purely gluonic operators ("glueballs") as dynamical degrees of freedom turns out to be non trivial [2–5]. In [2,4,5] the Veneziano-Yankielowicz low energy Lagrangian was extended so as to include all the desired low energy states, which are arranged into two Wess-Zumino supermultiplets. The authors of [3] pointed out on the other hand, that fulfillment of the program requires dynamical SUSY breaking and its consequent absence from the particle spectrum. In a situation where the theoretical framework seems to be still unsettled, a first-principles approach is welcome. This can be provided by lattice computations.

Our goal is to verify the low energy spectrum of SYM in the case of SU(2) gauge group by numerical techniques. By doing this we continue past projects, see [6] for a review. The direct approach to the spectrum of SYM consists in studying the time-dependence of correlators of operators having the expected quantum numbers of the low-lying particles. The simplest operators of this type are the glueball, gluino-glue and mesonic operators also entering the low energy Lagrangians. Since gluino bilinears and glueball operators of the same parity carry the same (conserved) quantum numbers of the theory, it is natural to expect mixing among them [2]. We have to stress here that when the dynamics of the gluinos is taken into account beyond the valence picture, the disentanglement of the "unmixed" states with identical quantum numbers is not possible: only the mixed physical states can be the object of investigation.[1] The result is the determination of the mass of the lightest particle with the same quantum numbers of the projecting operator: from this point of view glueball and mesonic operators are equivalent.

The action is discretized in the Wilson fashion [7][2] where, however, the gluino is a Majorana spinor in the adjoint representation:

$$S = S_G[U] + S_f\left[U, \bar{\lambda}, \lambda\right] \; ; \tag{1}$$

[a] e-mail: farchion@uni-muenster.de

[1] In order to avoid confusion with the mass pattern of QCD we refrain to associate any name to the particle states of SYM and will refer to them according to their quantum numbers (spin and parity).

[2] First simulations with domain wall fermions were performed in [8].

$S_G[U]$ is the usual plaquette action and

$$S_f\left[U,\bar\lambda,\lambda\right] = \frac{1}{2}\sum_x \bar\lambda(x)\lambda(x) - \frac{\kappa}{2}\sum_x\sum_\mu\left[\bar\lambda(x+\hat\mu)V_\mu(x)(r+\gamma_\mu)\lambda(x) + \bar\lambda(x)V_\mu^T(x)(r-\gamma_\mu)\lambda(x+\hat\mu)\right]; \qquad (2)$$

r is the Wilson parameter set to $r = 1$ in our case. The gluino field satisfies the Majorana condition

$$\lambda = \lambda^{\mathcal{C}} = \mathcal{C}\bar\lambda^T\,, \qquad (3)$$

where the charge conjugation in the spinorial representation is $\mathcal{C} = \gamma_0\gamma_2$; the gauge link in the adjoint representation reads:

$$[V_\mu(x)]_{ab} \equiv 2\,\mathrm{tr}[U_\mu^\dagger(x)T^aU_\mu(x)T^b] = \left[V_\mu^*(x)\right]_{ab} = \left[V_\mu^T(x)\right]_{ab}^{-1}\,, \qquad (4)$$

where T^a are the generators of the color group.

The dynamics of the gluinos is included by adopting the two-step multi-bosonic algorithm (TSMB) for dynamical fermions [9]. The algorithm has the nice feature of accommodating any, even fractional, number of flavors. This is required for SYM since, schematically, the gluino has only half of the degrees of freedom of a Dirac fermion and consequently the fermion measure contains the square root of the fermion determinant: this corresponds to $N_f = 1/2$. In addition (cf. [10] for details) the design of TSMB is optimized to deal with light fermionic degrees of freedom, a critical factor when approaching the SUSY limit. Tests of the algorithm performance in QCD for light quark masses can be found in [11].

In the Wilson discretization SUSY is broken in a twofold way: explicitly by the Wilson term ensuring the correct balance between fermionic and bosonic degrees of freedom in the continuum limit, and softly by the gluino mass term. On the basis of the Ward identities [7, 12, 13], SUSY is expected to be recovered in the continuum limit by tuning the gluino mass to zero. (The situation is perfectly analogous to that of QCD, where chirality is recovered by tuning the quark mass to zero). However, $O(a)$ and $O(m_{\tilde g})$ SUSY violating effects are expected to distort the SUSY pattern in practical situations. A systematic analytical expansion in the gluino mass is missing in SYM; therefore it is not obvious how to set the scale for the $O(m_{\tilde g})$ breaking (something analogous to $\Lambda_\chi = 4\pi f_\pi$ in chiral perturbation theory). The only possibility, at least for the moment, to gain some information on the effective "heaviness" of the gluino is to force analogy with QCD. Needless to say, this procedure is only of heuristic value. The strategy we adopt is to gradually increase the hopping parameter κ in the Wilson action at fixed value of the gauge coupling $\beta = 2.3$ corresponding to a fairly small lattice size in QCD units ($a \approx 0.06$ fm), pushing the simulation towards a lighter and lighter gluino.

First large scale simulations of SYM were performed in [10] on a $12^3\cdot 24$ for $\kappa = 0.1925$. New sets of configurations were produced in [13] for $\kappa = 0.194$, 0.1955. We now turn to a $16^3\cdot 32$ lattice, whose larger time extension allows for a better analysis of the spectrum. We consider here $\kappa = 0.194$ (simulations at $\kappa = 0.1955, 0.196$ are in progress). The larger space extension allows us to monitor finite-volume effects in the spectrum.

The spectrum of SYM is challenging from the point of view of numerical analysis. The signal for the correlators of purely gluonic operators vanishes very rapidly (ideally one should use anisotropic lattices). The mixed gluonic-fermionic operators, typical for SUSY models, receive substantial fluctuations from the gluonic content. A better asymptotic behavior of the effective mass, however, can be obtained by combined smearing of the fermionic and gluonic degrees of freedom. Finally for mesonic operators, special techniques are required for the disconnected term in the correlator. Here we employ stochastic estimators (SET) [14]. Also, we apply an improved version [15] of the volume source technique (VST) [16]. For fermions in the real representation of the gauge group, as is the case for SYM, the original formulation in [16] cannot be used. The two independent techniques were tested in a comparative study for SYM in [15].

A description and some results of this study have been reported in [17].

The plan of the paper is as follows. In Sect. 2 we report details of the simulations and characterize the gauge sample, using analogy with QCD, by the Sommer scale parameter r_0 and the pseudo-pion mass; the gluino mass is obtained from the soft-breaking term in the SUSY Ward identities; Sect. 3 contains methodology and results for the spectrum; in Sect. 4 we discuss results and indicate possible directions of improvement.

2 The gauge sample

The gauge configurations were generated by the two-step multi-bosonic algorithm for dynamical gluinos [9]. We refer to [10] for a description of the algorithm. Table 1 reports an overview of the $\beta = 2.3$ ensembles used in this work; the set on the $16^3\cdot 32$ lattice with $\kappa = 0.194$ was newly generated. The setup of the TSMB was as follows. The local part of the updating procedure (one cycle) consisted of two steps of heat bath for the bosonic fields followed by two steps of over-relaxation; the updating for the gauge sector was obtained by 36 Metropolis sweeps. At the end of each cycle an accept-reject test was performed on the gauge configuration, along the lines of the general procedure described in [10]. Every five cycles a global heat-bath step was applied on the bosonic fields. The typical condition number of the squared hermitian fermion matrix was $\sim 10^4$. The integrated autocorrelation time for the smallest eigenvalue was ~ 240 cycles.

2.1 Static potential, string tension and Sommer scale parameter

We measured the potential between heavy sources in the fundamental representation. The results on the larger $16^3\cdot$

Table 1. Overview of the ensembles used in this work with determination of Sommer scale parameter and string tension. The fourth and fifth column, respectively, report the total number of configurations and of update cycles at equilibrium, the sixth column the number of replica lattices

reference	L_s	κ	N_{config}	N_{cycle}	N_{lat}	r_0/a	$a\sqrt{\sigma}$
[10]	8	0.19	20768	1038400	32	5.41(28) [10]	0.22(1)
[10]	12	0.1925	4320	216000	9	6.71(19) [13]	0.176(4)
[13]	12	0.194	2034	42030	9	7.37(30) [13]	0.160(6)
this study	16	0.194	3890	25650	4	7.16(25)	0.165(9)
[13]	12	0.1955	4272	65832	8	7.98(48) [13]	0.147(8)

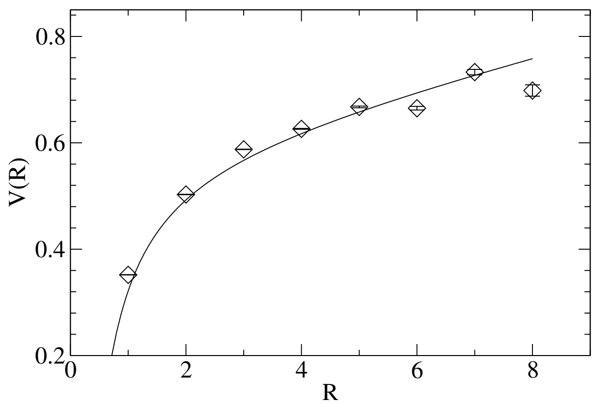

Fig. 1. Static potential between heavy sources in the fundamental representation on the $16^3 \cdot 32$ lattice, $\kappa = 0.194$; the line is the fit with lattice formulae

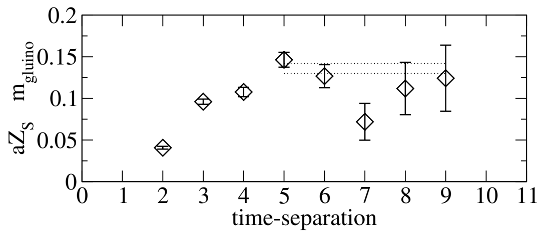

Fig. 2. The gluino mass as obtained from the SUSY Ward identities as a function of the time separation between current and insertion operator on the $16^3 \cdot 32$ lattice, $\kappa = 0.194$. The lines indicate bounds of the fit

32 lattice confirm the picture of confinement found in [10], see Fig. 1. The Sommer scale parameter r_0 and the string tension $\sqrt{\sigma}$ were measured by fitting the potential with the lattice formula [18]

$$V(\mathbf{r}) = V_0 + \sigma r - 4\pi e \int_{-\pi}^{\pi} \frac{\mathrm{d}^3 k}{(2\pi)^3} \frac{\cos(\mathbf{k}\cdot\mathbf{r})}{4\sum_{j=1}^{3}\sin^2(k_j/2)}\ ; \quad (5)$$

r_0 is given by

$$r_0 = \sqrt{\frac{1.65 - e}{\sigma}}\ . \quad (6)$$

The results are reported in Table 1.

Comparing the results on the two lattices, no finite-size effect beyond statistical uncertainty is visible in the Sommer scale parameter and the string-tension. Similarly to QCD, the Sommer scale parameter displays a sizeable gluino-mass dependence. A linear extrapolation to zero gluino mass is performed in the next subsection.

2.2 Massless gluino limit

In QCD the massless quark limit can be determined by inspection of the pion mass or use of the chiral Ward identities. In contrast, in SYM the $U(1)$ chiral symmetry is anomalous and the particle with the quantum numbers of the chiral current (namely the pseudoscalar particle) picks up a mass by the anomaly. However, theoretical arguments [1] (cf. also the discussion in [12]) support the picture that the anomaly is originated by OZI-rule violating diagrams, while the remaining ones determine spontaneous breaking of the chiral symmetry. The diagrams of the pseudoscalar correlator respecting the OZI-rule give rise to the connected (one loop) term, corresponding in QCD to the pion-correlator. The analogy with QCD suggests the name "adjoint-pion" ($a-\pi$) for the associated pseudoparticle: in the above picture this is expected to be a soft-mode of the theory, the corresponding mass disappearing for $m_{\tilde{g}} \to 0$.

The gluino mass can be directly determined by studying the lattice SUSY Ward identities [7,12,13], where the former enters the soft breaking term. We refer to [13] for the illustration of the method and discussion of theoretical aspects. One can determine the combination $aZ_S^{-1}m_{\tilde{g}}$ where Z_S is the renormalization constant of the SUSY current, which is expected to be a (finite) function of the gauge coupling only. This quantity was determined in [13] for the $12^3 \cdot 24$ lattice. We repeat here the computation for the $16^3 \cdot 32$ lattice. The results are reported in Fig. 2, where the gluino mass is plotted against the time separation between current and insertion operator in the SUSY Ward identities. Compared to the $12^3 \cdot 24$ case of [13], the plateau establishes for larger values of the time separation (five compared to three); unfortunately, at these time separations the quality of the signal is already quite deteriorated. Table 2 contains the determinations of $aZ_S^{-1}m_{\tilde{g}}$ and $am_{a-\pi}$ in present and past works. Comparison of $12^3 \cdot 24$ and $16^3 \cdot 32$ results at $\kappa = 0.194$ reveals a sizeable finite volume effect for the adjoint-pion mass. It should be noted that the sign of the effect is opposite to the usual one (however this is no physical mass). The gluino mass comes in larger on the larger lattice, however within a 1-σ effect.

Table 2. Quantities determined in this and previous studies: the adjoint-pion mass, gluino mass from SUSY Ward identities (with local SUSY current, insertion operator $\chi^{(sp)}$, cf. Table 5 in [13]), spin-1/2, 0^+ and 0^- bound state masses

L_s	κ	$am_{a-\pi}$	$aZ_S^{-1}m_{\tilde{g}}$	spin-1/2	0^+(glueb.)	$0^-(\bar{\lambda}\gamma^5\lambda)$
8	0.19	0.71(2) [10]				
12	0.1925	0.550(1)	0.166(6) [13]	0.33(4)	0.53(10) [20]	0.52(10) [20]
12	0.194	0.470(4)	0.124(6) [13]	0.49(4)	0.40(11)	0.42(1)
16	0.194	0.484(1)	0.137(7)	0.43(1)		0.52(2)
12	0.1955	0.253(4)	0.053(4) [13]	0.35(4)	0.36(4)	0.24(2)

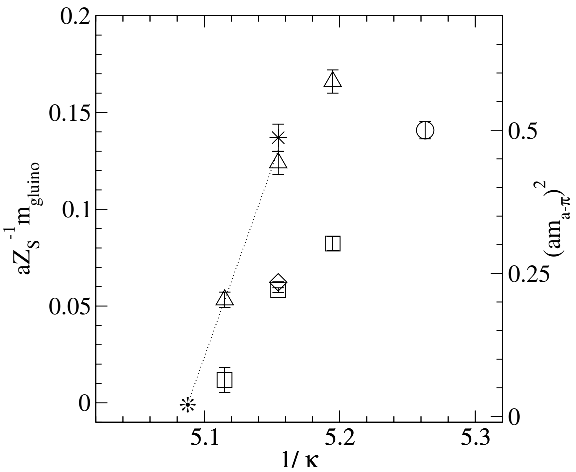

Fig. 3. The gluino mass from the SUSY Ward identities and the squared adjoint-pion mass $m_{a-\pi}$ as a function of $1/\kappa$ (from the present and past studies [10,13]); $aZ_S^{-1}m_{\tilde{g}}$ on the $12^3 \cdot 24$ lattice (triangles), the same quantity on the $16^3 \cdot 32$ lattice (star); squared adjoint-pion mass on $8^3 \cdot 16$ (circle), $12^3 \cdot 24$ (boxes), and $16^3 \cdot 32$ lattice (diamond). The burst indicates the extrapolated massless limit from the two lightest gluino masses

In Fig. 3 $aZ_S^{-1}m_{\tilde{g}}$ is shown together with the squared adjoint-pion mass. The two quantities appear to vanish for a common value of $\kappa \equiv \kappa_c$. The estimate of κ_c from the SUSY Ward identity gluino mass, $\kappa_c \approx 0.1965$ [13], is not changed by the inclusion of the point on the larger lattice. Using this value of κ_c we can now extrapolate the Sommer scale parameter in Table 1 to the massless gluino situation. A linear extrapolation results in $r_0/a(m_{\tilde{g}} = 0) = 8.4(4)$; the error takes into account the uncertainty in the determination of κ_c (assumed to be in the region κ=0.1965–0.1975 [13]). The Sommer scale parameter signals the degree of "smoothness" (or "coarseness") of the gauge sample. In QCD, the present value would correspond to $a \approx 0.06$ fm (3.3 GeV), a fairly fine lattice. Further, assuming that the adjoint-pion drives the low energy features of SYM, as the pion does in QCD, one can estimate the degree of soft-breaking of SUSY by considering the dimensionless quantity $M_r = (m_{a-\pi}r_0)^2$. In QCD, validity of NLO chiral perturbation theory requires [21] a $M_r \lesssim 0.8$ (corresponding to $m_{ud} \lesssim 1/4\, m_s$). In our case we have $M_r(\kappa = 0.194) \approx 16$ and $M_r(\kappa = 0.1955) \approx 4.5$; our lightest case would correspond in QCD to $m_{ud} \approx 1.5\, m_s$. Alternatively one can consider the gluino mass from the SUSY Ward identity neglecting $O(1)$ renormalizations, again fixing the scale by the Sommer parameter with QCD units. In this case we obtain for our lightest gluino $m_{\tilde{g}} \approx 174$ MeV in rough agreement with the previous estimate. Since QCD and SU(2) SYM are different theories, the above indications are of course of qualitative nature. On the other hand, the relatively large average condition numbers of the fermion matrix, $\sim 10^4$ for $\kappa = 0.194$ and $\sim 3.6\ 10^4$ for $\kappa = 0.1955$, point towards a lighter gluino.

3 The spectrum

As explained above, we concentrate our analysis of the spectrum on particles with spin = 0 (both parities) and spin = 1/2. We investigate the glueball operators, the gluino scalar and pseudoscalar bilinears (meson-type operators) and the gluino-glue operator.

3.1 Spin-1/2 bound states

We adopt here a lattice version [13] of the gluino-glue operator $\mathrm{tr}_c[F\sigma\lambda]$ where the field-strength tensor $F_{\mu\nu}(x)$ is replaced by the clover-plaquette operator $P_{\mu\nu}(x)$:

$$\mathcal{O}^{\alpha}_{\tilde{g}g}(x) = \sum_{i<j} \sigma^{\alpha\beta}_{ij}\ \mathrm{tr}_c \left[P_{ij}(x)\lambda^{\beta}(x)\right] \ ; \tag{7}$$

only spatial indices are taken into account in order to avoid links in the time-direction. The clover-plaquette operator is defined to be

$$P_{\mu\nu}(x) = \frac{1}{8ig_0} \sum_{i=1}^{4} \left(U^{(i)}_{\mu\nu}(x) - U^{(i)\dagger}_{\mu\nu}(x) \right) \tag{8}$$

with

$$\begin{aligned}
U^{(1)}_{\mu\nu}(x) &= U^{\dagger}_{\nu}(x)U^{\dagger}_{\mu}(x+\hat{\nu})U_{\nu}(x+\hat{\mu})U_{\mu}(x) \\
U^{(2)}_{\mu\nu}(x) &= U^{\dagger}_{\mu}(x)U_{\nu}(x-\hat{\nu}+\hat{\mu})U_{\mu}(x-\hat{\nu})U^{\dagger}_{\nu}(x-\hat{\nu}) \\
U^{(3)}_{\mu\nu}(x) &= U_{\nu}(x-\hat{\nu})U_{\nu}(x-\hat{\nu}-\hat{\mu}) \\
&\quad \times U^{\dagger}_{\mu}(x-\hat{\nu}-\hat{\mu})U^{\dagger}_{\mu}(x-\hat{\mu}) \\
U^{(4)}_{\mu\nu}(x) &= U_{\mu}(x-\hat{\mu})U^{\dagger}_{\nu}(x-\hat{\mu})U^{\dagger}_{\mu}(x+\hat{\nu}-\hat{\mu})U_{\nu}(x) \,.
\end{aligned} \tag{9}$$

The choice of the clover plaquette vs. the regular plaquette as the gluonic field-strength operator in (7) is motivated by the correct behavior under parity and time reversal transformations as opposed to simply $U_{\mu\nu}(x)$. Because of the spinorial character of the gluino-glue, the correlator $C_{\tilde{g}g}(t)$ has a specific structure in Dirac space. On the basis of the symmetries of the theory, one can show [12] that only two components are linearly independent, $\mathrm{tr}_D[C_{\tilde{g}g}(x)]$ and $\mathrm{tr}_D[\gamma_0 C_{\tilde{g}g}(x)]$. In our experience, the latter gives the best signal. In order to get a better overlap with the ground state, we apply APE smearing [22] on the link-variables and Jacobi smearing [23] on the gluino field simultaneously.

3.2 0^- bound states

The meson-type correlators require a separate discussion because of the disconnected contribution. In the case of SYM one has (with Δ the gluino propagator):

$$\begin{aligned} C_{\mathrm{meson}}(x_0-y_0) &= C_{\mathrm{conn}}(x_0-y_0) - C_{\mathrm{disc}}(x_0-y_0) \\ &= \frac{1}{V_s}\sum_{\boldsymbol{x}} \langle \mathrm{tr}[\Gamma \Delta_{x,y} \Gamma \Delta_{y,x}]\rangle \qquad (10) \\ &\quad - \frac{1}{2V_s}\sum_{\boldsymbol{x}} \langle \mathrm{tr}[\Gamma \Delta_{x,x}]\, \mathrm{tr}[\Gamma \Delta_{y,y}]\rangle \;, \end{aligned}$$

with $\Gamma \in \{1, \gamma_0\}$ (observe the factor 1/2 reflecting the Majorana nature of the gluino). The disconnected term requires the estimation of the time-slice sum of the gluino propagator

$$S_{\alpha\beta}(x_0) = \sum_{\boldsymbol{x}} \mathrm{tr}_c[\Delta_{x\alpha,x\beta}]\,. \qquad (11)$$

For this, we use the stochastic estimator technique (SET) [14] with complex Z_2 noise in the spin explicit variant SEM [19]. In this case each estimate of the time-slice sum is obtained by inverting the fermion-matrix with source $(\omega_S^{[\alpha]})_{xb\beta} = \delta_{\alpha\beta}\,\eta_{xb}^{[\alpha]}$ where $\eta_{xb}^{[\alpha]}$ are independent stochastic variables chosen at random from $\frac{1}{\sqrt{2}}(\pm 1 \pm i)$. Here we use point-like operators (i.e., no smearing on the gluino).

On the larger $16^3 \cdot 32$ lattice the computed meson correlator displays an offset: its long-time behavior is not purely exponential, since a constant term also appears. Such a constant term is theoretically excluded in the correlator by the symmetries of the theory. It is present in both SET and VST (see below) determinations of the disconnected contribution and does not decrease by increasing the number of the random estimators. In contrast, it is absent in the connected correlator. We conclude that its origin is to be traced to some cumulative numerical effect in the stochastic computation of the disconnected contribution.

In Fig. 4 we show the disconnected component of the pseudoscalar meson correlator after subtraction of the constant term. In Fig. 5 the ratio between the subtracted disconnected component and the connected one is reported. For a comparison with the same quantity in the case of QCD see e.g., [24,25]; we remark here that the case of SYM is quite different since the connected correlator is not related to a physical particle, but rather to the pseudoparticle $a - \pi$ discussed above.

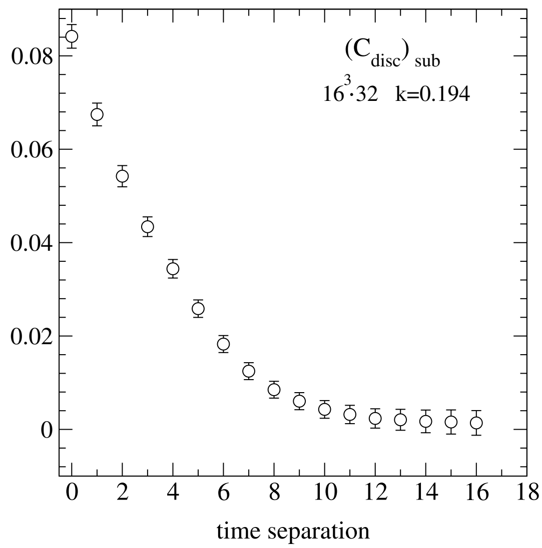

Fig. 4. The disconnected component of the pseudoscalar meson correlator after subtraction of the constant term on the $16^3 \cdot 32$ lattice, $\kappa = 0.194$ (SET)

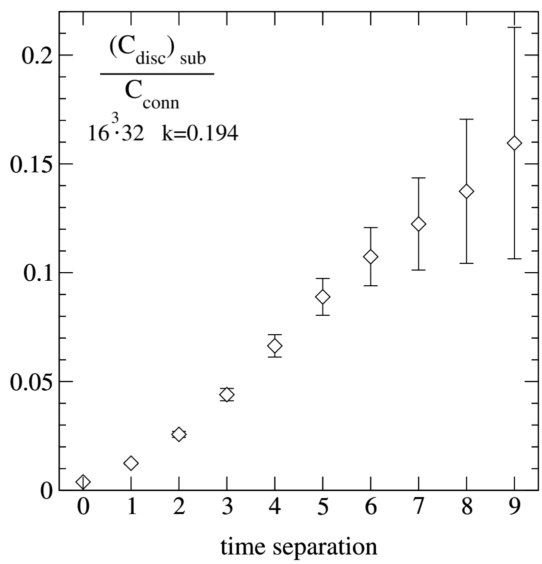

Fig. 5. Ratio of the disconnected (after subtraction) and connected components of the pseudoscalar meson correlator on the $16^3 \cdot 32$ lattice, $\kappa = 0.194$ (SET)

We cross-check the SET with the improved version [15] of the volume source technique (VST) [16], applying to fermions in real representations of the color group. The improvement consists in averaging the time-slice sums over random gauge transformations and therefore eliminating the gauge non-invariant spurious terms. The two methods deliver consistent results of comparable quality at similar computational cost. For the sake of brevity, we present here only those from SET.

Another operator with the right quantum numbers (0^-) is the pseudoscalar glueball operator. This is given by a linear combination of closed loops of link variables which cannot be rotated into their mirror image (cf. e.g., [10]). We considered the simplest loops of this kind. Unfortunately this operator does not give a clear signal on our samples.

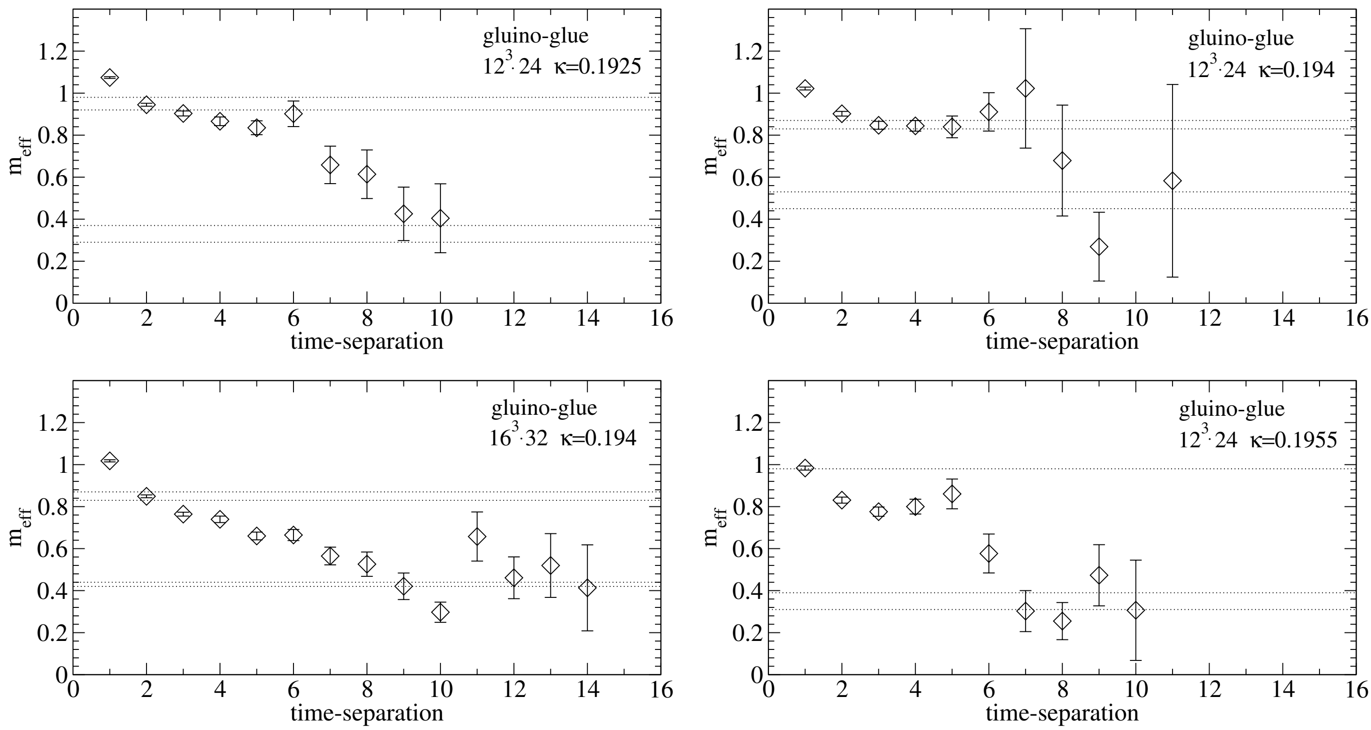

Fig. 6. The effective mass of the spin-1/2 particle (γ_0 component) for the different samples. Dotted lines are the bounds of the mass fits (ground and first excited state). In the last case only a rough indication of the first excited state mass could be obtained

3.3 0^+ bound states

Since the meson-type correlator does not show any appreciable signal for the 0^+ state, we turn to the scalar glueball operator. The standard operator in this case is

$$\mathcal{O}_{\mathrm{glueball}}(x) = \mathrm{tr}_c[U_{12}(x) + U_{23}(x) + U_{31}(x)] \,. \qquad (12)$$

We use fuzzy operators by applying APE smearing on the link variables.

3.4 Results

For all particles we measured the effective masses (Figs. 6–8). In many cases a clear plateau could not be determined. In order to get a better determination of the ground state mass, we used constrained two-mass fits (bounds in the figures). In some cases (the spin-1/2 particle on the larger lattice at $\kappa = 0.194$, Fig. 6, and the pseudoscalar particle at the same κ value, Fig. 7) the two-mass fit can be cross-checked against a plateau of the effective mass. We ensured the stability of the two-mass fits by systematically varying fit ranges (for details see [17]). The effective mass of the pseudoscalar meson on the $16^3 \cdot 32$ lattice, lower panel of Fig. 7, was determined after subtraction of the constant term in the correlator discussed in Sect. 3.2.

In the case of the scalar glueball operator, a decrease of the signal/noise ratio was observed on the larger lattice, as a consequence of which no determination of the mass was possible.

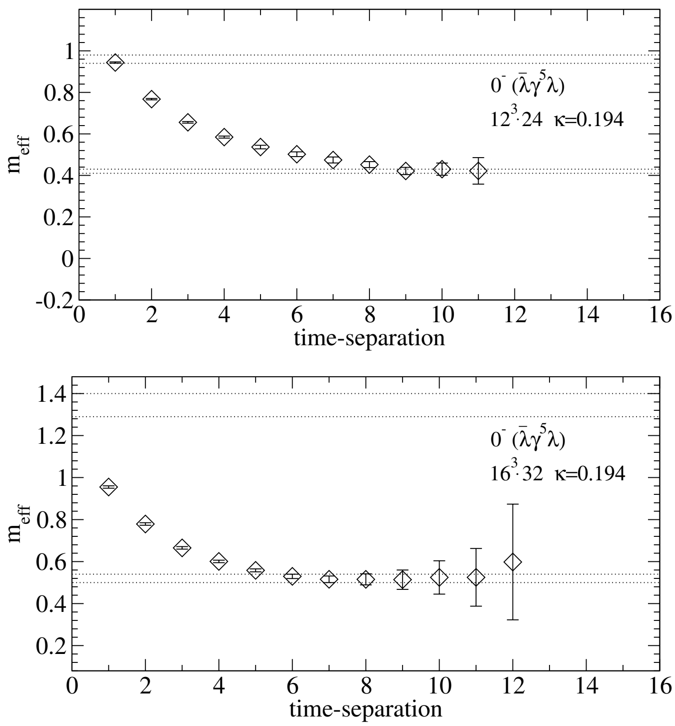

Fig. 7. The comparison of the effective mass of the pseudoscalar particle on the two lattices at $\kappa = 0.194$. Dotted lines are the bounds of the mass fits (ground and first excited state)

Results on the determinations of the ground state masses are reported in Table 2 and Fig. 9. A discussion of the results will be presented in the following section.

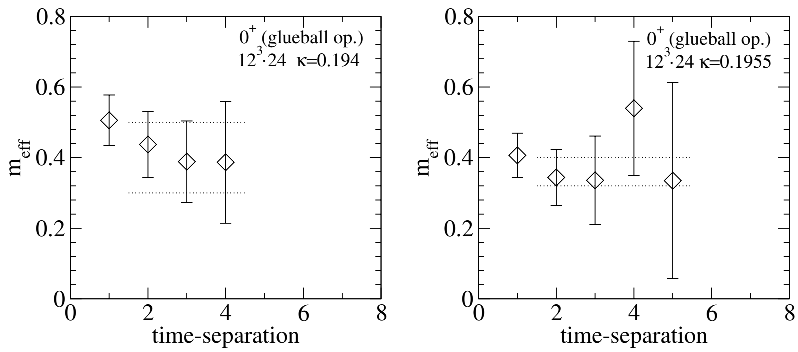

Fig. 8. The effective mass of the scalar particle with glueball operator on the $12^3 \cdot 24$ lattice at $\kappa = 0.194, 0.1955$. Dotted lines are the bounds of one-mass fits

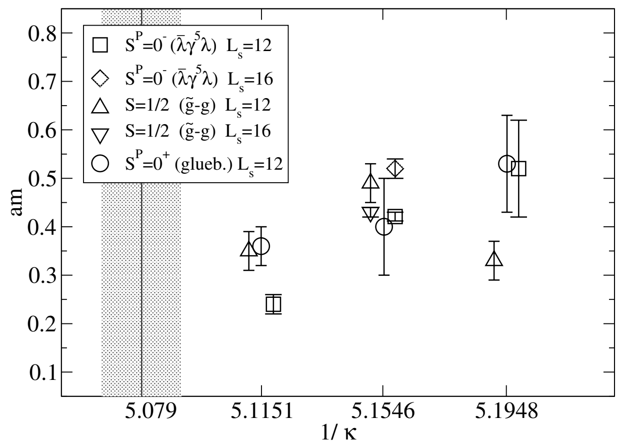

Fig. 9. Mass of lightest bound states of SYM determined in this work. The shaded region represents the presumed location of the massless gluino on the basis of the SUSY Ward identity analysis

4 Discussion

Our analysis of the low-lying spectrum of SYM shows a slow approach of the correlators to the asymptotic behavior where only the ground state dominates. This is evident in the case of the gluino-glue and mesonic correlators; in the case of the glueball correlator, the quality of the signal is not good enough to make definite statements. Excited states with masses comparable to that of the ground state are strongly coupled to these operators. In some cases a plateau of the effective mass emerged and consequently allowed us to cross-check the results of the two-mass fits. The situation can be improved by implementing optimized smearing on the operators (in the case of the gluino bilinears we use point-like operators).

The excited states which hamper the determination of the ground states are of physical interest by themselves. According to [2, 4, 5], the first excited states should be arranged in a second Wess-Zumino supermultiplet. The "higher masses" in our two-mass fits can give a first indication of the masses of these excited states: the ground state masses lie in the region 0.2–0.5 (in lattice units), while the higher masses are in the region 0.8–1. A more refined analysis of the excited states, however, could be obtained with matrix correlators. In the scalar sector, one would naturally include the gluino scalar bilinear in addition to the glueball operator. Given the large fluctuations observed on the former, the employment of variational methods would then be advisable. A similar analysis could be done in the pseudoscalar sector with the corresponding gluino bilinear and the pseudoscalar glueball operator.

A more fundamental question is whether the employed operators are optimal in the sense of maximal overlap with the low-lying bound states of SYM. Investigations could go in the direction of different operators and different quantum numbers [26].

In the following we restrict the discussion of our results to the ground states (Fig. 9). One of the goals of this study was to check finite volume effects by comparing lattices with different spatial extension. This can be done for our value of $\kappa = 0.194$ where two different lattice sizes are available, $L_s = 12$ and 16. The direct comparison shows, see Table 2, that a sizeable deviation is present for the pseudoscalar particle. Contrary to expectations, the particle comes in heavier on the larger lattice. For this lattice, however, an unexpected constant term is observed in the long-time behavior of the correlator, which could hint at some systematic effect in the stochastic determination of the disconnected correlator on large lattices. The pseudoscalar particle is the lightest particle for our lightest gluino ($\kappa = 0.1955$), though, in this case only data for the smaller lattice are available. The scalar and the spin-1/2 particle have comparable masses, compatible within errors.

Conclusions on the relevance of soft breaking terms require the control of finite lattice-spacing effects. Using analogy with QCD in absence of other indications, we argue that our mesh is relatively fine, while the gluino is still quite heavy. Next steps will be therefore to consider larger values of κ on large lattices.

Acknowledgements. We thank C. Gebert for participating in the early stages of this work, I. Montvay and G. Münster for stimulating discussions. The computations were performed on the Cray T3E and JUMP systems at NIC Jülich, the PC clusters at the ZIV of the University of Münster and the Sun Fire SMP-Cluster at the Rechenzentrum of the RWTH Aachen.

References

1. G. Veneziano, S. Yankielowicz, Phys. Lett. B **113**, 231 (1982)
2. G.R. Farrar, G. Gabadadze, M. Schwetz, Phys. Rev. D **58**, 015009 (1998)

3. L. Bergamin, P. Minkowski, hep-th/0301155
4. D.G. Cerdeno, A. Knauf, J. Louis, Eur. Phys. J. C **31**, 415 (2003)
5. P. Merlatti, F. Sannino, hep-th/0404251; A. Feo, P. Merlatti, F. Sannino, hep-th/0408214
6. I. Montvay, Int. J. Mod. Phys. A **17**, 2377 (2002)
7. G. Curci, G. Veneziano, Nucl. Phys. B **292**, 555 (1987)
8. G. Fleming, J. Kogut, P. Vranas Phys. Rev. D **64**, 034510 (2001)
9. I. Montvay, Nucl. Phys. B **466**, 259 (1996); Comput. Phys. Commun. **109**, 144 (1998)
10. I. Campos, A. Feo, R. Kirchner, S. Luckmann, I. Montvay, G. Münster, K. Spanderen, J. Westphalen, Eur. Phys. J. C **11**, 507 (1999)
11. F. Farchioni, C. Gebert, I. Montvay, L. Scorzato, Eur. Phys. J. C **26**, 237 (2002)
12. A. Donini, M. Guagnelli, P. Hernandez, A. Vladikas, Nucl. Phys. B **523**, 529 (1998)
13. F. Farchioni, A. Feo, T. Galla, C. Gebert, R. Kirchner, I. Montvay, G. Münster, A. Vladikas, Eur. Phys. J. C **23**, 719 (2002)
14. S.J. Dong, K.F. Liu, Phys. Lett. B **328**, 130 (1994)
15. F. Farchioni, G. Münster, R. Peetz, Eur. Phys. J. **C** (in press), hep-lat/0404004
16. Y. Kuramashi, M. Fukugita, H. Mino, M. Okawa, A. Ukawa, Phys. Rev. Lett. **72**, 3448 (1994)
17. R. Peetz, Ph.D. Thesis, University of Münster, 2003
18. R.G. Edwards, U.M. Heller, T.R. Klassen, Nucl. Phys. B **517**, 377 (1998)
19. J. Viehoff et al. [SESAM Collaboration], Nucl. Phys. Proc. Suppl. **63**, 269 (1998)
20. R. Kirchner, Ph.D. Thesis, University of Hamburg, 2000
21. S.R. Sharpe, N. Shoresh, Phys. Rev. D **62**, 094503 (2000)
22. M. Albanese et al., Phys. Letters B **192**, 163 (1987)
23. C.R. Allton et al. [UKQCD Collaboration], Phys. Rev. D **47**, 5128 (1993)
24. T. Struckmann et al. [TXL Collaboration], Phys. Rev. D **63**, 074503 (2001)
25. V.I. Lesk et al. [CP-PACS Collaboration], Phys. Rev. D **67**, 074503 (2003)
26. K. Johnson, Diploma Thesis, University of Münster, 2002; H. Schmalle, Diploma Thesis, University of Münster, 2004